Distinct α-Synuclein Strains Differentially Promote Tau Inclusions in Neurons

Jing L. Guo,[1] Dustin J. Covell,[1] Joshua P. Daniels,[1] Michiyo Iba,[1] Anna Stieber,[1] Bin Zhang,[1] Dawn M. Riddle,[1] Linda K. Kwong,[1] Yan Xu,[1] John Q. Trojanowski,[1] and Virginia M.Y. Lee[1,*]

[1]Department of Pathology and Laboratory Medicine, Institute on Aging and Center for Neurodegenerative Disease Research, University of Pennsylvania School of Medicine, Philadelphia, PA 19104, USA

*Correspondence: vmylee@upenn.edu

http://dx.doi.org/10.1016/j.cell.2013.05.057

SUMMARY

Many neurodegenerative diseases are characterized by the accumulation of insoluble protein aggregates, including neurofibrillary tangles comprised of tau in Alzheimer's disease and Lewy bodies composed of α-synuclein in Parkinson's disease. Moreover, different pathological proteins frequently codeposit in disease brains. To test whether aggregated α-synuclein can directly cross-seed tau fibrillization, we administered preformed α-synuclein fibrils assembled from recombinant protein to primary neurons and transgenic mice. Remarkably, we discovered two distinct strains of synthetic α-synuclein fibrils that demonstrated striking differences in the efficiency of cross-seeding tau aggregation, both in neuron cultures and in vivo. Proteinase K digestion revealed conformational differences between the two synthetic α-synuclein strains and also between sarkosyl-insoluble α-synuclein extracted from two subgroups of Parkinson's disease brains. We speculate that distinct strains of pathological α-synuclein likely exist in neurodegenerative disease brains and may underlie the tremendous heterogeneity of synucleinopathies.

INTRODUCTION

A common feature of many neurodegenerative diseases is the accumulation of normally soluble proteins into filamentous insoluble aggregates. Examples include tau neurofibrillary tangles (NFTs) in Alzheimer's disease (AD) and frontotemporal degeneration (reviewed by Lee et al., 2001) and α-synuclein (α-syn) Lewy bodies (LBs) in Parkinson's disease (PD) and dementia with LB (DLB) (reviewed by Goedert et al., 2013). Whereas tau is a microtubule-binding protein that stabilizes and promotes microtubule assembly in axons (Witman et al., 1976), α-syn is a phospholipid-binding protein concentrated in presynaptic terminals where it promotes SNARE complex formation and modulates synaptic functions (Burré et al., 2010; Murphy et al., 2000). Although the mechanisms whereby tau and α-syn aggregates induce neurodegeneration are not understood, they are thought to contribute to neuronal dysfunction and death through loss of normal functions and/or toxic gains of functions (reviewed by Ballatore et al., 2007; Goedert, 2001).

Both tau and α-syn are natively unfolded soluble proteins without well-defined secondary or tertiary structures (Weinreb et al., 1996), but how they undergo conformational changes to become insoluble and form aggregates is unclear. Recently, increasing evidence supports robust aggregation of tau and α-syn induced by exogenously supplied preformed fibrils (pffs) in cultured cells, as well as in living animals, suggesting that small amounts of misfolded protein can act as seeds to initiate templated recruitment of their soluble counterparts into fibrils (Frost et al., 2009; Guo and Lee, 2011; Iba et al., 2013; Luk et al., 2009, 2012a, 2012b; Volpicelli-Daley et al., 2011). Moreover, cell-to-cell transmission of these amyloid protein aggregates may underlie the stereotypical spatiotemporal progression of both AD and PD pathologies (reviewed by Jucker and Walker, 2011).

Another recurrent theme of neurodegenerative diseases is the frequent co-occurrence of different disease protein aggregates in the same patient. For example, >50% of AD cases show LBs, whereas co-morbid AD pathologies, including Aβ plaques and NFTs, are commonly found in PD and DLB brains (reviewed by Galpern and Lang, 2006). One potential explanation is global dysregulation of protein homeostasis in disease brains, whereby misfolding of one major protein overwhelms the proteostatic machinery and compromises folding of other aggregation-prone proteins (reviewed by Kikis et al., 2010). Alternatively, filamentous aggregates composed of one protein may directly cross-seed other amyloidogenic proteins owing to potentially shared structural features of amyloid fibrils (Kayed et al., 2007; O'Nuallain and Wetzel, 2002). Indeed, we showed earlier that recombinant α-syn and tau proteins synergistically promote the fibrillization of each other in vitro (Giasson et al., 2003), whereas more recently, α-syn pffs were shown to induce tau aggregation in cultured non-neuronal cells (Waxman and Giasson, 2011). To confirm this cross-seeding phenomenon in physiologically more relevant systems, we utilized recently developed synucleinopathy models in primary neurons and transgenic (Tg)

mice, in which exogenously added α-syn pffs promote aggregation of endogenous α-syn (Luk et al., 2012b; Volpicelli-Daley et al., 2011). By using these models, we discovered two distinct "strains" of synthetic α-syn pffs with differential ability to cross-seed tau aggregation in cultured neurons and in vivo. In this work, we define strains as conformational variants of α-syn fibrils with differing cross-seeding properties in these cellular and organismal contexts.

RESULTS

Generation of Different Strains of α-Syn pffs with Differential Cross-Seeding of Tau

To investigate whether α-syn pffs cross-seed tau in primary neurons, we incubated hippocampal neurons from mouse embryos overexpressing human mutant P301S tau (PS19) with α-syn pffs assembled de novo from C-terminal-truncated 1–120 monomers with a Myc tag (1–120-Myc). At 18 days post-transduction, highly abundant LB and Lewy-neurite (LN) like α-syn inclusions that are resistant to Triton X-100 extraction were observed throughout the cultured neurons (Figure 1A, top panel). However, Triton-insoluble hyperphosphorylated tau aggregates were infrequent and rarely colocalized with α-syn pathology. The lack of direct evidence for physical interactions between α-syn and tau aggregates suggests that the formation of the latter is likely an indirect consequence of α-syn accumulation rather than a direct result of cross-seeding by α-syn. In neurons derived from non-Tg mice, no appreciable tau aggregates were induced (Figure 1A, bottom panel).

Remarkably, a very different pattern of Triton-insoluble α-syn and tau inclusions was observed in neurons treated with a preparation of 1–120-Myc pffs generated through repetitive seeded fibrillization in vitro, whereby 5% or 10% of pffs from each passage were included as seeds in the fibrillization reaction of the subsequent passage (Figure 1B). Although α-syn pathology was somewhat less abundant at 18 days post-transduction compared to transduction with de novo 1–120-Myc pffs, widespread fibrillar tau aggregates that extensively colocalized with neuritic α-syn inclusions were observed in both PS19 and non-Tg neurons (Figure 1C). Surprisingly, the extent of endogenous mouse tau pathology induced in non-Tg neurons by these α-syn pffs dramatically exceeded that induced by synthetic tau pffs (Guo and Lee, 2013). To distinguish these two distinct types of α-syn pffs that are reminiscent of prion "strains," we designate pffs that have limited cross-seeding ability of tau, which were used in all our previous α-syn transmission studies, as strain A, and the newly discovered pffs with efficient cross-seeding of tau as strain B (Luk et al., 2009, 2012b; Volpicelli-Daley et al., 2011) (Table S2 available online). Generation of strain B through repeated self-seeding in vitro was reproduced using several different batches of 1–120-Myc monomer, as confirmed by phenotypic transition from a relative paucity of insoluble tau in early passages to appearance of robust tau pathology in later passages (Figure S1A).

Although strain B α-syn pffs efficiently induce endogenous tau aggregation in non-Tg neurons, this phenomenon failed to occur in α-syn knockout neurons (Figure 1D), suggesting that endogenous mouse α-syn mediates fibrillization of mouse tau in non-Tg

neurons. It is conceivable that the internalized α-syn pffs themselves provide an insufficient quantity of nucleating structures to directly trigger tau fibrillization, presumably due to a less efficient cross-seeding of tau than homotypic seeding of α-syn, whereas endogenous α-syn aggregates templated by internalized pffs create additional seeding structures sufficient to initiate the conversion of soluble tau into aggregates.

To test whether wild-type (WT) full-length (FL) α-syn also forms strain A and B α-syn fibrils, non-Tg neurons were incubated for 18 days with FL α-syn pffs generated de novo (passage 1 or P1) or through repetitive self-seeding in vitro (P2 onward) (Figure 1B). P1 pffs always behaved as strain A, resulting in profuse α-syn inclusions with minimal tau aggregation (Figure 1E). FL α-syn pffs of subsequent passages led to diminishing α-syn pathology with small amounts of neuritic tau pathology first emerging in neurons transduced with P4 or P5 pffs, followed by full conversion to strain B that induced abundant tau pathology by P6-7 (Figure 1E). Such strain A to strain B conversion through repeated self-seeding in vitro was accomplished with four different batches of FL α-syn monomer, although this process did not always give rise to prototypical strain B pffs as defined above. An intermediate phenotype with relatively abundant tau pathology accompanied by far more abundant α-syn pathology was sometimes observed (Figure S1B); this is likely due to incomplete conversion of strain A to strain B resulting in a mixture of the two strains. Notably, continual self-seeding in vitro after full or partial conversion to strain B led to "strain drift" within a few passages, resulting in what we refer to as "post-B strains," which induce a variable amount of tau pathology and morphologically diverse α-syn inclusions (Figure S1C; Table S2).

Characterization of Neurons Transduced with Different Strains of α-Syn pffs

Immunoelectron microscopy (immuno-EM) in a previous study showed abundant phospho-α-syn-positive filaments throughout perikarya and processes of neurons transduced with α-syn pffs now designated as strain A (Volpicelli-Daley et al., 2011). Similarly, immuno-EM also detected cytoplasmic α-syn filaments in strain B pff-transduced neurons but mostly confined to neurites (Figures 2A and 2B). Meanwhile, filamentous aggregates immunoreactive for phospho-tau were observed in neurons treated with strain B pffs, confirming fibrillization of tau induced by heterotypic seeds (Figures 2C and 2D). Moreover, double-labeling immuno-EM of strain B-transduced neurons showed close physical associations of tau with α-syn in filamentous structures in neuronal processes (Figures 2E and 2F), strongly supporting direct physical templating as the primary mechanism for strain B α-syn pff-induced tau aggregation. The lack of tau immunoreactivity around occasional perikaryal α-syn-positive filaments indicates specificity of our double-labeling technique (Figure 2G).

Immunocytochemistry on neurons incubated for different durations with α-syn pffs generated from either FL or 1–120-Myc α-syn more clearly revealed differences between the two strains (Figures 3 and S2). Non-Tg neurons transduced with strain A pffs were replete with α-syn pathology in the absence of any tau pathology at 10 days post-transduction, but those transduced with strain B pffs showed only sparse α-syn aggregates, whereas
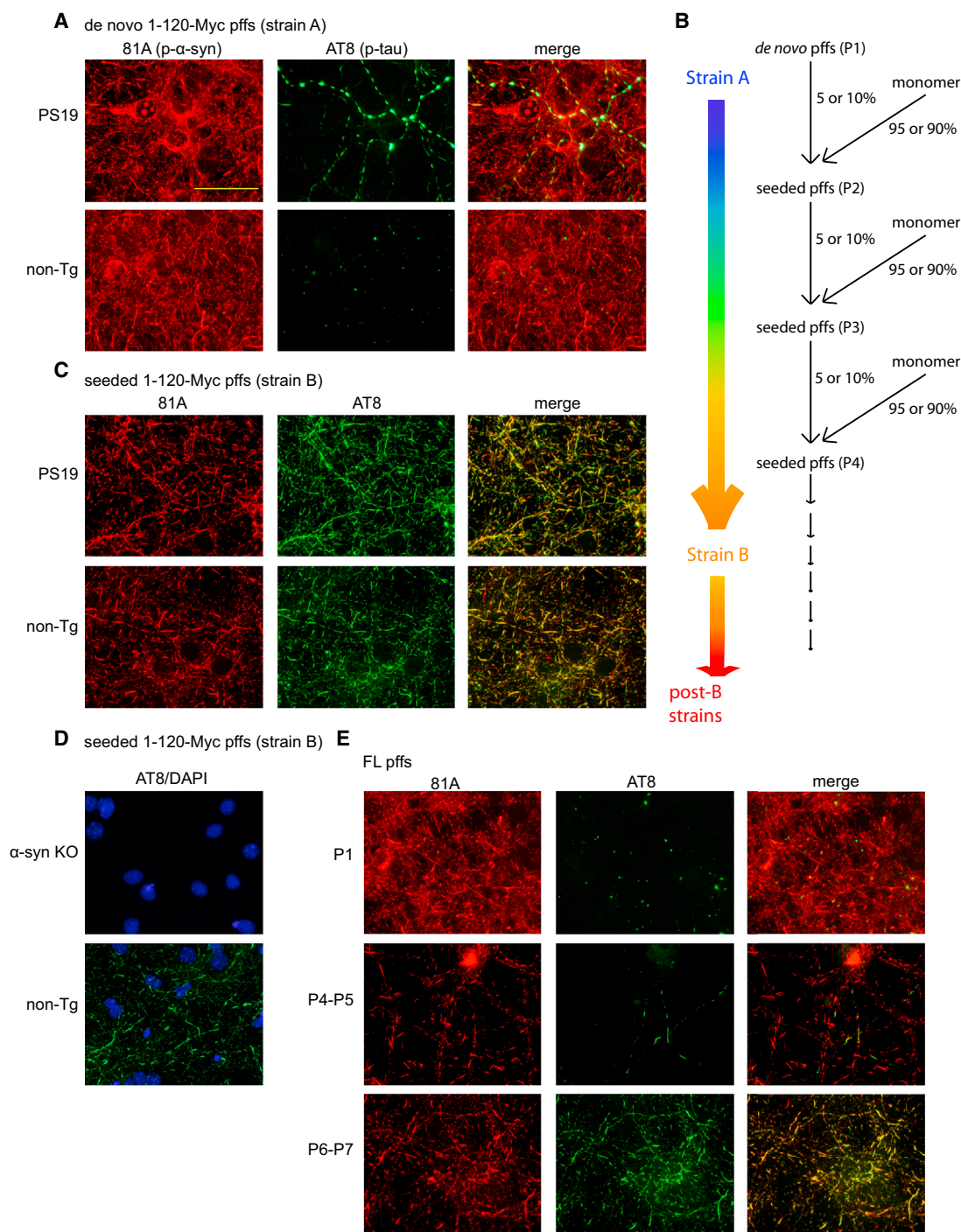
Figure 1. Generation of Different Strains of α-Syn pffs with Differential Cross-Seeding of Tau in Neurons

(A) Insoluble phospho-α-syn (81A) and phospho-tau (AT8) induced by de novo 1–120-Myc pffs (strain A) in primary hippocampal neurons dissociated from PS19 or non-Tg mouse embryos.

(B) Procedures of repetitive seeded fibrillization in vitro resulting in evolution of strain A pffs into B and post-B strains.

(C) α-syn and tau pathologies caused by seeded 1–120-Myc pffs (strain B) in PS19 and non-Tg neurons.

(D) Staining of insoluble phospho-tau (AT8, green) in α-syn knockout (α-syn KO) or non-Tg neurons transduced with strain B 1–120-Myc pffs. DAPI (blue) revealed cell nuclei.

(E) Phenotypic changes in α-syn and tau pathologies induced by FL α-syn pffs of different self-seeding passages.

For (A), (C), (D), and (E), neurons were fixed 18 days post-transduction, and soluble proteins were removed during fixation. Scale bar: 50 μm. See also Figure S1 and Table S2.
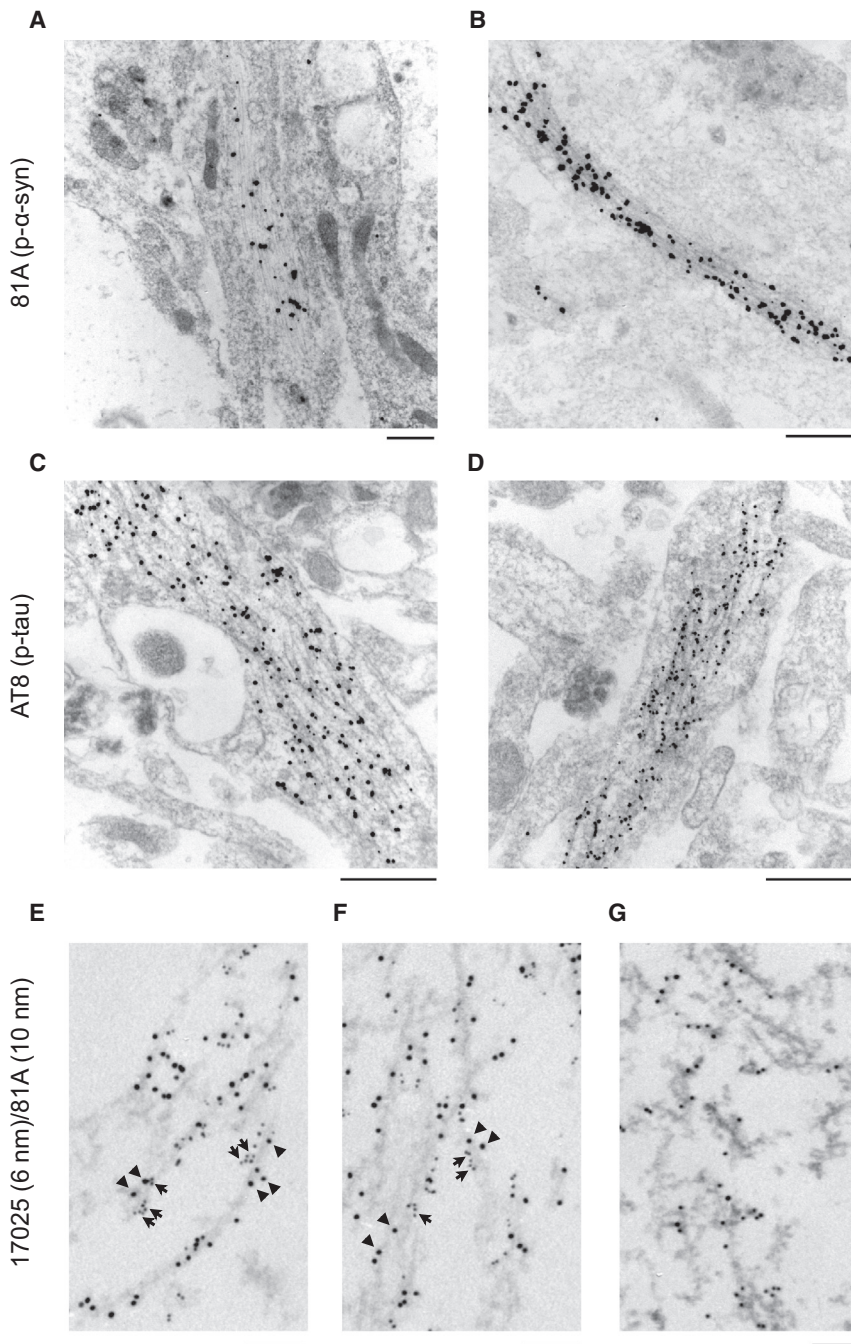
Figure 2. Ultrastructural Analysis of Strain B α-Syn pff-Induced Cytoplasmic Filaments by Immuno-EM

(A and B) 81A-immunoreactive α-syn filaments observed in strain B α-syn pff-transduced neurons labeled by nanogold.

(C and D) AT8-positive tau filaments in these neurons detected by nanogold.

(E–G) Double-labeling using 81A and 17025 (a pAb against tau) as primary antibodies followed by secondary antibodies conjugated to 10 nm colloidal gold (for α-syn) or 6 nm colloidal gold (for tau). (E) and (F) show filaments decorated by both α-syn (arrowheads) and tau (arrows) antibodies found in neurites, whereas (G) shows filaments almost exclusively composed of α-syn found in a cell body.

Scale bar: 500 nm for (A)–(D), 100 nm for (E)–(G).

seeding properties of the two strains of α-syn pffs. Triton-insoluble tau was only detected in strain B pff-transduced neurons, being most prominent after 18 days of incubation, even though Triton-insoluble α-syn was much more abundant in neurons treated with strain A pffs (Figures 3E, 3F, and S2B).

Consistent with our previous study (Volpicelli-Daley et al., 2011), strain A pffs were highly toxic to neurons as evidenced by significantly increased lactate dehydrogenase (LDH) release and reduced metabolic activity after 14 days of incubation (Figures 3G, S2C, and S2D). By contrast, strain B pffs had no negative impact on cell survival even after 18 days of incubation. Immunostaining of microtubule-associated protein 2 (MAP2) and neurofilament light chain (NFL) in 18 days post-transduction neurons showed bundled but intact neuronal processes in strain B-treated neurons, whereas a dramatic reduction in the density of both MAP2 and NFL and frequent beading of dendritic MAP2 were observed in strain A-treated neurons (Figure S2E). The prominent reduction of soluble tau in 18-day strain A-transduced neuron lysates was most likely a result of extensive cell death as well (Figures 3E, 3F, and S2B).

Biophysical and Biochemical Analyses of α-Syn pff Strains

To determine whether the distinct seeding properties of the two α-syn pff strains reflect structural differences, a series of biophysical and biochemical analyses were performed. First, negative-staining transmission EM (TEM) showed no convincing difference in the morphology of filaments (Figure S3A). Second,

small amounts of neuritic tau accumulations already emerged (Figures 3A and S2A). By 14 days and 18 days post-transduction, the burden of α-syn aggregates increased in strain B-transduced neurons, accompanied by a dramatic increase in tau aggregates, nearly all of which colocalized with α-syn pathology (Figures 3A–3D and S2A). In contrast, strain A-induced α-syn pathology appeared to plateau at 14 days post-transduction, but no neuritic tau pathology ever occurred. Immunoblotting of lysates from neurons that were sequentially extracted with 1% Triton X-100 lysis buffer followed by 2% SDS lysis buffer confirmed the distinct

ThT fluorescence signals of similar amounts of strain A and B fibrils demonstrated wide variability without clear separation (Figure S3B). Third, Fourier transform infrared spectroscopy (FTIR) and circular dichroism (CD) only showed minor differences between these two strains (Figures S3C and S3D), suggesting that structural differences between them are subtle.

To test whether α-syn pff strains can be distinguished biochemically using proteinase K (PK) digestion as demonstrated for human prion strains (Aguzzi et al., 2007; Parchi et al., 1996), different passages of FL α-syn pffs generated through self-seeding in vitro were incubated with PK at 37°C. The digestion products predominantly consist of five bands between 10 and 15 kDa, with the fifth band being least abundant for P1 pffs (Figure 4A). Notably, the fifth band consistently became highly prominent around P5–P7, correlating with the transition of strain A to strain B. The relative intensity of the fifth band compared to the first band typically shows a decline from P1 to P2, followed by an upward trend at later passages (Figure 4B), suggesting stereotypical conformational changes generated by repetitive seeded fibrillization.

To directly examine whether the two strains of pffs show distinct PK digestion patterns, neuronal phenotype-confirmed strain A and B pffs were incubated with different concentrations of PK (Figure 4C). No significant difference in overall PK resistance was observed, such that no loss in the total amount of α-syn proteins was seen after each strain was treated with PK (Figure S3E). The first band of the PK digestion products presumably represents residual uncleaved FL α-syn pffs as it comigrates with FL α-syn on denaturing gels. Detailed analysis of all five bands revealed a significantly higher ratio of cleaved species (sum of second to fifth bands) to uncleaved α-syn (first band) for strain B pffs at all PK concentrations (Figure 4D). This difference was predominantly driven by increased relative abundance of the third and fifth bands in the strain B digestion products, with the fifth band most dramatically differentiating the two strains at 2.5 μg/ml PK (Figures 4E, 4F, S3F, and S3G).

N-terminal sequencing indicated that both the second and fourth bands primarily contain α-syn peptides starting around residues 19–21, whereas the third and fifth bands both start at residue 31 (Figure 4A). Taking into account epitope mapping with a panel of antibodies specific to domains spanning the entire α-syn molecule (Figure 4G), we deduced the identities of the major PK digestion products (Figure 4H). Both the third and fifth bands, which are more prominent in PK-digested strain B pffs, consist of peptides N-terminally cleaved after residue 30, whereas the fifth band has an additional C-terminal cleavage site around residue 125 (Figure 4H). Increased N- and C-terminal truncation of strain B pffs by PK suggests that the two termini may be more exposed for PK access in strain B than in strain A pffs. Moreover, the two strains of pffs made from 1–120-Myc, which lacks the C-terminal cleavage site for PK, were clearly distinguished by an elevated amount of PK digestion product starting at residue 31 for strain B (Figure S3H), further supporting increased PK cleavage at the N terminus as a biochemical signature for strain B pffs.

To further confirm that the two strains of α-syn pffs are conformational variants, we generated a monoclonal antibody (mAb), 9029-03, which displays ~3-fold selectivity for strain B pffs

over strain A pffs as quantified by enzyme-linked immunosorbent assay (ELISA) (Figure 4I). This strain B-selective antibody demonstrated an inverted U-shape curve of immunoreactivity for different passages of α-syn pffs within each self-seeded propagation series, consistent with the emergence of strain B conformers after repetitive self-seeding and later conversion to post-B strains (Figure 4J).

The Roles of N and C Termini in Strain Conformations

Because possible conformational changes of α-syn pffs at the N and C termini correlate with phenotypic conversion from strain A to B, we tested self-seeded pffs assembled from N- or C-terminal-truncated α-syn molecules to determine whether the two termini play causal roles in strain evolution (Figure 5A; Table S3). Interestingly, pffs made from N-terminal-truncated α-syn 58–140 and 32–140 almost always remained incapable of cross-seeding tau up to P10 of self-seeding despite efficient induction of α-syn pathology (Figure 5B). The N terminus of α-syn thus appears necessary for generating in the exogenous α-syn pffs a cross-seeding-competent conformation that can be conferred through templating onto endogenous α-syn, which is required for recruiting tau (Figures 1D and 5A). Besides the lack of tau cross-seeding, both 58–140 and 32–140 pffs remained phenotypically stable in terms of α-syn pathology induced by different passages of pffs in neurons. Whereas 32–140 pffs constantly behaved as strong strain A pffs, 58–140 pffs invariably led to morphologically distinct α-syn aggregates, consisting of unusually long fibrillar accumulations in neurites with almost no cell-body inclusions (Figure 5B). Interestingly, when templated by 58–140 pffs in vitro, FL α-syn pffs are also capable of acquiring similar seeding properties in neurons (Figure S4A), thus pointing to a unique conformation adopted by 58–140 pffs that can be acquired by FL α-syn.

The similar behavior of 1–120-Myc and FL α-syn in strain evolution suggests that the extreme C terminus may play a minimal role in pff conformation. Surprisingly, 1–120 without a myc tag at the C terminus stochastically gave rise to different strains of de novo pffs with no predictable pattern of strain conversion through repetitive self-seeding (Figure S4B). Therefore, unlike the N terminus of α-syn, which appears to contribute to conformational diversity of fibrils, the C terminus seems to impede structural diversity. The more predictable behavior of 1–120-Myc may be due to enriched negative charges in the Myc tag, which may partially mimic the natural C terminus of FL α-syn.

To test whether the N and C termini are an integral part of strain-specific conformations, or merely facilitating the acquisition of distinct conformations by middle regions of α-syn, N- or C-terminal-truncated α-syn proteins were fibrillized in the presence of 10% strain A or strain B pffs to test their ability to conform to these respective strains when seeded (Figure 5A; Table S3). For strain A-seeded fibrillization, an additional round of self-seeding was conducted to dilute out the original strain A seeds. 1–120 α-syn faithfully acquired strain A phenotype when seeded by strain A pffs (Figures 5C and S4C), suggesting that the extreme C terminus is not an essential part of strain A conformation. In contrast, strain A-seeded 58–140 pffs still predominantly induced elongated α-syn accumulations with infrequent cell-body inclusions (Figures 5C and S4C). Therefore, the absence
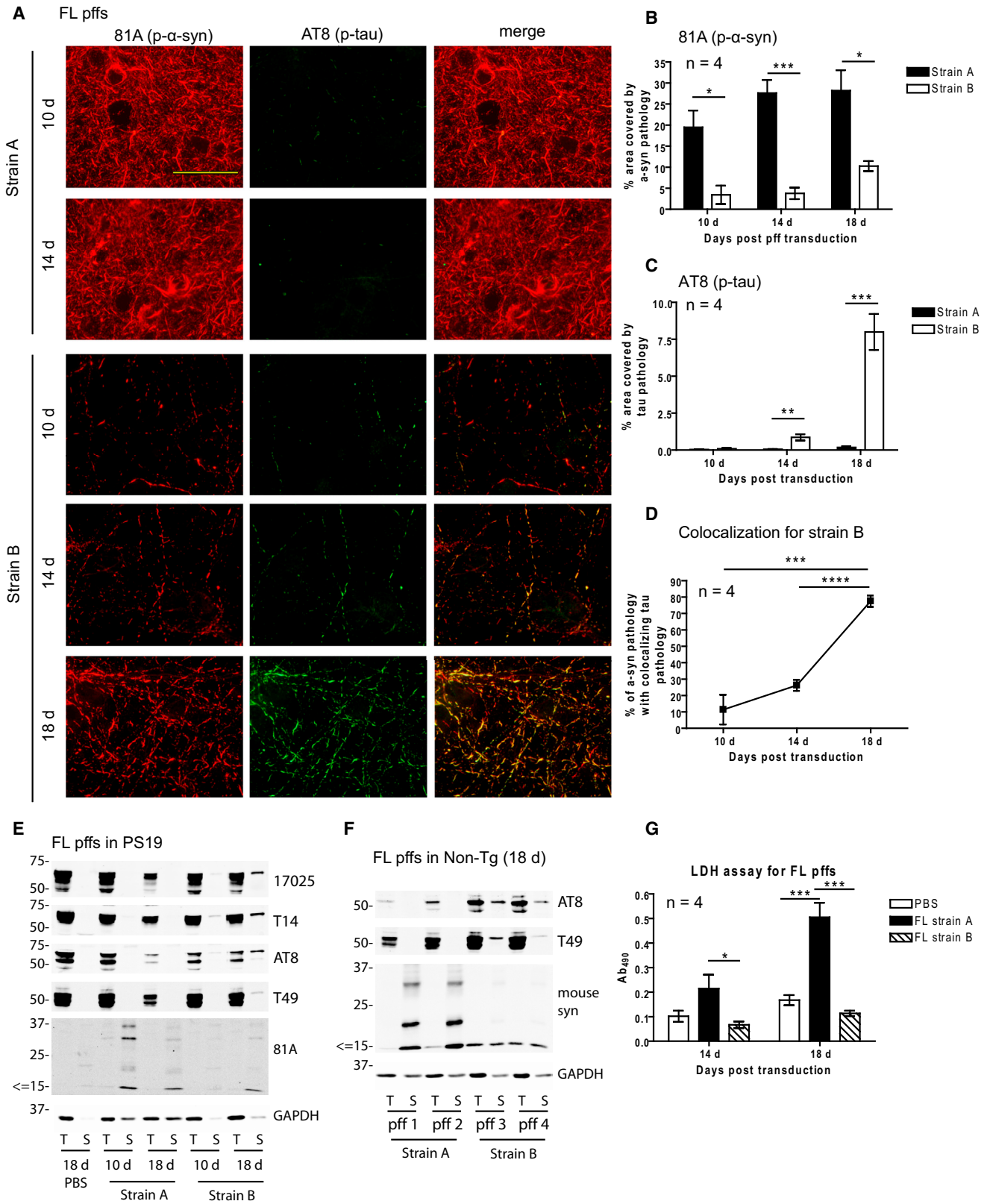
(legend on next page)

of residues 1–57 impairs the acquisition of strain A conformation. As expected from the spontaneous generation of strain A pffs, 32–140 pffs seeded by strain A always displayed typical strain A phenotypes (data not shown), confirming that residues 1–31 are not an integral part of strain A core structure. This in turn points to residues 32–57 as an important region of α-syn needed to adopt the strain A configuration.

When seeded by strain B pffs, FL α-syn, 32–140, and 1–120 all reliably acquired the ability to induce tau aggregation far beyond what could be attributed to the 10% strain B seeds present in the fibrillization mixture (Figures 5D, 5E, and S4D). The extensive colocalization between endogenous α-syn and tau pathology (Figures 5D and 5F) further supports the induction of specific endogenous α-syn conformers that are capable of cross-seeding tau. Therefore, although the initial 31 residues at the extreme N terminus and the last 20 residues at the C terminus may facilitate the spontaneous generation of strain B by FL α-syn through repetitive self-seeding, they do not constitute the core structure of the strain B conformation. However, we did notice significantly less-abundant aggregation of both α-syn and tau induced by strain B-seeded 32–140 and 1–120 than by equivalently seeded FL α-syn pffs (Figure 5E). This suggests that the lack of the extreme N or C terminus of α-syn may result in reduced efficiency in strain B-templated fibrillization. On the other hand, strain B-seeded 58–140 pffs still behaved exactly the same as spontaneously generated 58–140 pffs, with the sparsely distributed tau inclusions entirely accounted for by the 10% residual strain B seeds (Figures 5D, 5E, and 5F), thereby indicating a complete failure to adopt the strain B conformation. The striking difference between 32–140 and 58–140 when seeded by strain B further implicates the critical role of residues 32–57 in the generation of the strain B conformation as well.

Strain-Specific Cross-Seeding of Tau Pathology In Vivo

To test whether the two strains of α-syn pffs can differentially induce tau pathology in vivo, we performed unilateral inoculation of strain A or B α-syn pffs into the hippocampus of 2- to 3-month-old PS19 mice, which overexpress human P301S mutant tau, prior to the onset of extensive transgene-induced tau pathology at ∼12 months of age (Iba et al., 2013). The induction and spreading of tau and α-syn inclusions were examined with immunohistochemistry at different time points after α-syn pff inoculation. At 3 months post-injection, only rare cells showed abnormal accumulation of hyperphosphorylated tau recognized by mAb AT8 near the injection site of strain A-inoculated mice, whereas numerous neurons bearing AT8-positive tau inclusions were observed in strain B-injected mice around the same area (Figures 6A and 6B). Moreover, strain B-injected mice not only displayed significantly more tau inclusions in all parts of the hippocampus, including regions that are more rostral and caudal to the injection site (Figures 6A and 6B), but also consistently showed phospho-tau aggregates in the contralateral hippocampus and even locus coeruleus, a brainstem structure distant from the injection site (Figure S5A), indicating transmission of tau pathology cross-seeded by α-syn pffs. The differential induction of tau aggregates by the two strains of pffs was confirmed with MC1, a mAb specific for a pathological conformation of tau (Jicha et al., 1997) (Figure 6C). Further characterization revealed that tau aggregates cross-seeded by α-syn pffs were also recognized by TG3, a conformational-specific phospho-tau mAb, and Ac-K280, a polyclonal antibody (pAb) specific for acetylated tau (Figure 6D), thus distinguishing them from spontaneously developed tau pathology in aged PS19 mice (Iba et al., 2013).

At 6 months post-injection, strain B pff-inoculated mice continued to show significant tau pathology, although there was only a minor increase in the rostral and caudal hippocampus and even a slight reduction of pathology around the injection site as compared to 3 month post-injection mice. In contrast, strain A-injected mice demonstrated an obvious increase in phospho-tau aggregates at 6 and 9 months post-injection, but the extent of tau pathology in mice receiving strain A was far less than that induced by strain B even at 9 months post-injection (Figures 6A and 6B). These results clearly illustrate the greatly enhanced tau cross-seeding capacity of strain B pffs compared to strain A pffs in living animals, exactly as observed in cultured neurons.

Curiously, tau pathology in α-syn pff-injected PS19 mice occurred without substantial α-syn pathology, as only a small number of cells bearing distinct α-syn inclusions were found in the caudal hippocampus, regardless of strains of pffs injected (Figures S5B and S5C). The relatively low efficiency of α-syn pathology induction by human α-syn pffs (both strains A and B), contrasting with our earlier study of mouse α-syn pff inoculation into non-Tg mice (Luk et al., 2012a), could be due to a partial species barrier that is not obvious in the less stringent cell culture system. The overexpression of human mutant tau in PS19 mice appears to overcome the reliance on α-syn pathology in templating tau aggregation when tau is not overexpressed

Figure 3. Inverse Seeding Capacity for α-Syn and Tau Pathologies Accompanied by Differential Cellular Toxicity

(A) Insoluble phospho-α-syn (81A) and phospho-tau (AT8) in non-Tg neurons at different days post-transduction with strain A or strain B FL α-syn pffs. Soluble proteins were removed during fixation.

(B and C) Quantification of % area occupied by 81A- and AT8-labeled pathologies, respectively, for experiments described in (A) (results shown as mean ± standard error of the mean [SEM]. *p < 0.05; **p < 0.01; ***p < 0.0005).

(D) Calculation of % of α-syn pathology with colocalizing tau pathology (area occupied by 81A/area occupied by AT8 × 100%) for strain B pff-transduced neurons (results shown as mean ± SEM. ***p < 0.0005; ****p < 0.0001).

(E) PS19 neurons treated with PBS or transduced with strain A or strain B FL α-syn pffs were sequentially extracted with 1% Triton X-100 lysis buffer (T) followed by 2% SDS lysis buffer (S) at different time points. Neuron lysates from T and S fractions were immunoblotted with 17025 (total tau), T14 (human tau), AT8 (phospho-tau), T49 (mouse tau), 81A (phospho-α-syn), and GAPDH antibody (loading control).

(F) Non-Tg neurons at 18 days post-transduction of strain A or strain B FL α-syn pffs were sequentially extracted and immunoblotted with AT8, T49, mouse α-syn, and GAPDH antibodies.

(G) LDH assay on differently treated non-Tg neurons at 14 days and 18 days post-transduction (results shown as mean ± SEM. *p < 0.05; ***p < 0.005).

Scale bar: 50 μm. See also Figure S2.
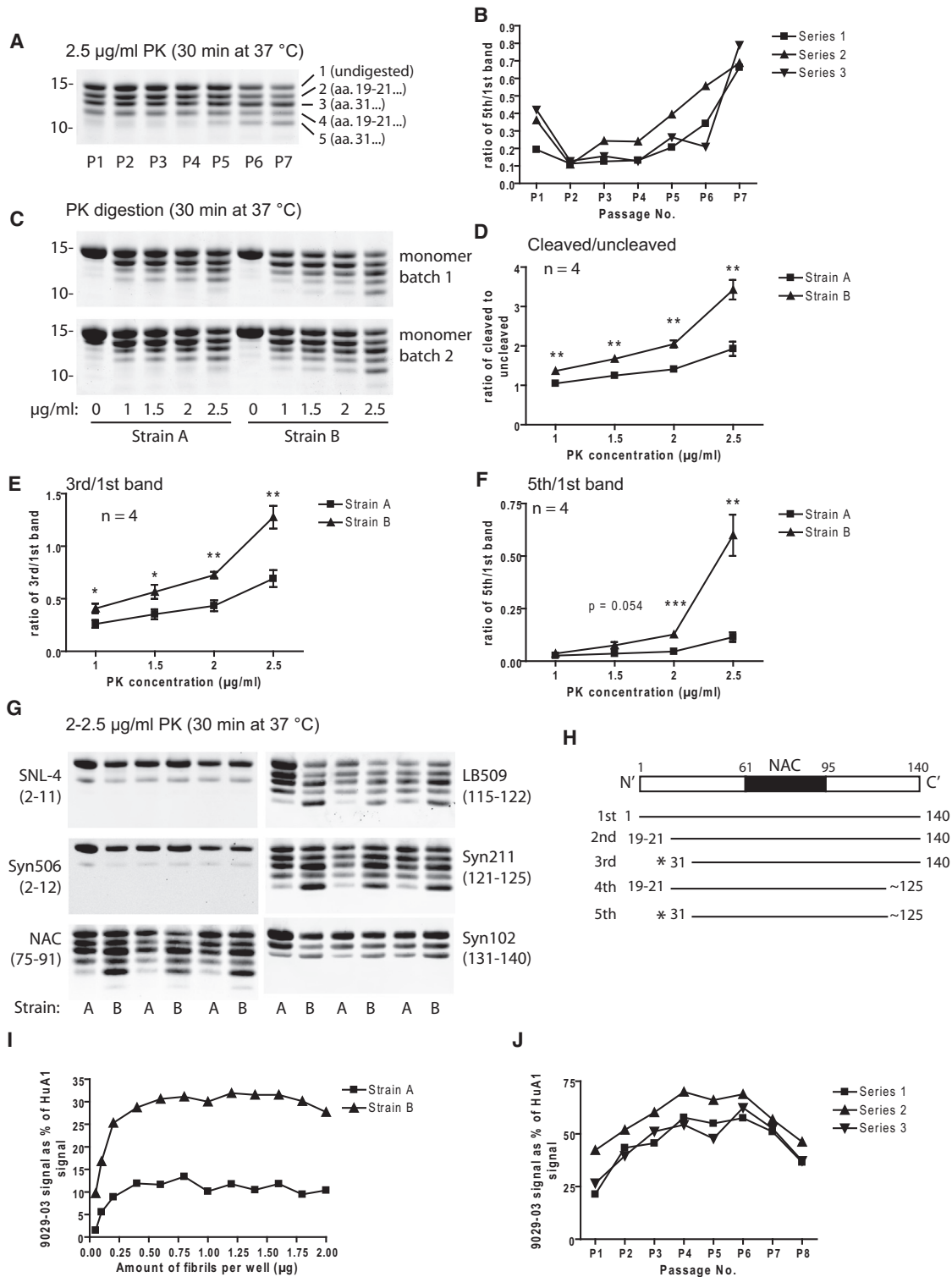
Figure 4. Conformational Differences between the Strains Revealed by PK Digestion and a Strain-Selective Antibody

(A) Different passages (P1–P7) of self-seeded FL α-syn pffs were digested with PK, resolved on 12% Bis-Tris gel, and stained with Coomassie blue. Results from one representative series are shown. N-terminal sequencing results for the 2nd to 5th bands are presented in parentheses.

(B) Quantification of the relative intensity of the 5th band to the 1st band for experiments described in (A) for three series of self-seeded FL α-syn pffs.

(C) Pairs of strain A and B FL α-syn pffs made from the same batches of monomer were incubated with different concentrations of PK (1–2.5 μg/ml). Digestion products from two pairs of pffs were shown. Untreated pffs were loaded on the same gels (0 μg/ml).

(legend continued on next page)

(Figure 1D), which can account for failed induction of tau pathology in non-Tg mice receiving hippocampal injection of either strain of α-syn pffs up to 6 months post-injection (data not shown).

Conformational Variations of Pathological α-Syn in Human Brains

To assess pathological α-syn strains in human synucleinopathy brains, we performed biochemical analysis on five cases of PD with dementia (PDD), three of which had a secondary neuropathological diagnosis of AD due to abundant NFTs and senile plaques (Figure 7A). For all five cases, immunoblots on sarkosyl-insoluble fraction from the cingulate gyrus showed salient α-syn bands (Figure 7B). Although all five cases showed varying amounts of sarkosyl-insoluble tau, it was much more abundant in cases 3 and 4, which had higher NFT scores (Figures 7A and 7C). Interestingly, upon PK digestion of sarkosyl-insoluble fraction, two distinct banding patterns of α-syn were observed. The two relatively "pure" PDD cases (cases 1 and 2) showed only one prominent band running at ∼15 kDa, whereas the three PDD cases with a secondary diagnosis of AD (cases 3–5) demonstrated two prominent PK-resistant bands at ∼16 and ∼14 kDa. These results suggest that at least two conformational variants of pathological α-syn exist in PDD brains, but the sample size at this stage is too small to correlate strain conformations with pathological manifestation.

DISCUSSION

Our study demonstrates that distinct synthetic α-syn strains with different cross-seeding tau properties can be generated in vitro. Experiments on 32–140 and 1–120 α-syn revealed that both N and C termini facilitate the stereotypical conversion of strain A into strain B with continual seeding, although they themselves are not part of the core structure for either strain. Previous structural studies suggest that the fibrillization core of α-syn spans residues 30 to ∼100–110 (Comellas et al., 2011; Miake et al., 2002; Vilar et al., 2008), extending beyond the NAC domain (residues 61–95) that is both necessary and sufficient for α-syn fibrillization (Giasson et al., 2001). Although 58–140 with an intact NAC domain is fully capable of seeding endogenous α-syn fibrillization, a unique pathological conformer distinct from strain A or B was generated, supporting the structural role of residues on the N-terminal side of the NAC domain in regulating α-syn fibril conformations. Moreover, compared with 32–140, 58–140 is deficient in acquiring either strain A or B conformation when seeded (Table S3), suggesting that residues 32–57 constitute a

critical part of the fibrillization core for both strains and the exact folding of this region within fibrillar α-syn strongly influences its seeding properties in neurons, consistent with a high-resolution solid-state nuclear magnetic resonance (NMR) study showing that the β strand consisting of residues 38–49 displays more dynamic structure than other β strands in the fibril core (Comellas et al., 2011).

The concept of "strains" originated from the prion field, whereby prion variants are associated with characteristic histopathological lesion profiles and different clinical manifestations that are believed to be encoded by conformational differences in the infectious prion particles (reviewed by Aguzzi et al., 2007). The different synthetic α-syn conformers we describe here closely parallel prion strains in that they exhibit structural variations, differences in seeding properties, and heritability of phenotypic traits via direct seeding in vitro. Our demonstration that a spectrum of α-syn strains can arise from the simplest reactions in a cell-free system without any cofactors suggests that in real human brains with a highly complex cellular and biochemical environment, the likelihood of forming diverse strains may be far greater. Interestingly, LBs found in midbrain structures such as the substantia nigra are morphologically different from those found in the cortical regions (Spillantini et al., 1998), possibly representing distinct strains of α-syn aggregates formed under specific cellular milieus. Moreover, in PDD or DLB cases with concomitant AD pathologies, NFTs are more frequently detected in limbic and neocortical areas than in midbrain (Gearing et al., 1999; Gómez-Tortosa et al., 2000). This region-specific distribution of co-occurring NFTs could be due to selective vulnerability of different brain areas to tau aggregation, but it could also result from differential cross-seeding capacity of α-syn aggregates arising in these different regions. In fact, close physical association of tau and α-syn deposits are frequently observed in synucleinopathies (Duda et al., 2002; Ishizawa et al., 2003; Kotzbauer et al., 2004), supporting direct cross-seeding between the two types of pathologies.

Besides differing cellular and biochemical factors, other events can also facilitate the generation of different α-syn strains in vivo. First, C-terminally truncated α-syn has been detected in synucleinopathy brains (Baba et al., 1998; Li et al., 2005). This cleavage event can accelerate fibrillization of α-syn (Murray et al., 2003) and also promote stochastic formation of diverse aggregated strains as shown here. Second, recent studies have implicated interneuronal transmission of α-syn aggregates as the underlying mechanism for stereotypical progression of α-syn pathology in PD and DLB. Because every transmission event from one neuron to the other can be viewed as a bona fide seeded

(D) Quantification of the ratio of cleaved species (sum of the 2nd to 5th bands) to uncleaved molecules (the 1st band) for experiments described in (C) (results shown as mean ± SEM. **p < 0.01).

(E) Quantification of the ratio of the 3rd band to the 1st band for the same samples as in (D) (results shown as mean ± SEM. *p < 0.05; **p < 0.01).

(F) Quantification of the ratio of the 5th band to the 1st band for the same samples as in (D) (results shown as mean ± SEM. **p < 0.01; ***p < 0.001).

(G) PK-digested FL α-syn pffs were immunoblotted with antibodies recognizing different epitopes of α-syn, indicated in parentheses.

(H) Deduced identities of major products from PK digestion.

(I) Different amounts of strain A or B FL α-syn pffs (0.05 to 2 μg) coated on an ELISA plate were incubated with HuA1, a pAb raised against recombinant human α-syn, and 9029-03, our newly generated strain B-selective mAb.

(J) Different passages of FL α-syn pffs immobilized on an ELISA plate were probed with HuA1 and 9029-03. Results from three series are shown.

For (I) and (J), absorbance for 9029-03 was expressed as % of absorbance for HuA1. See also Figure S3.
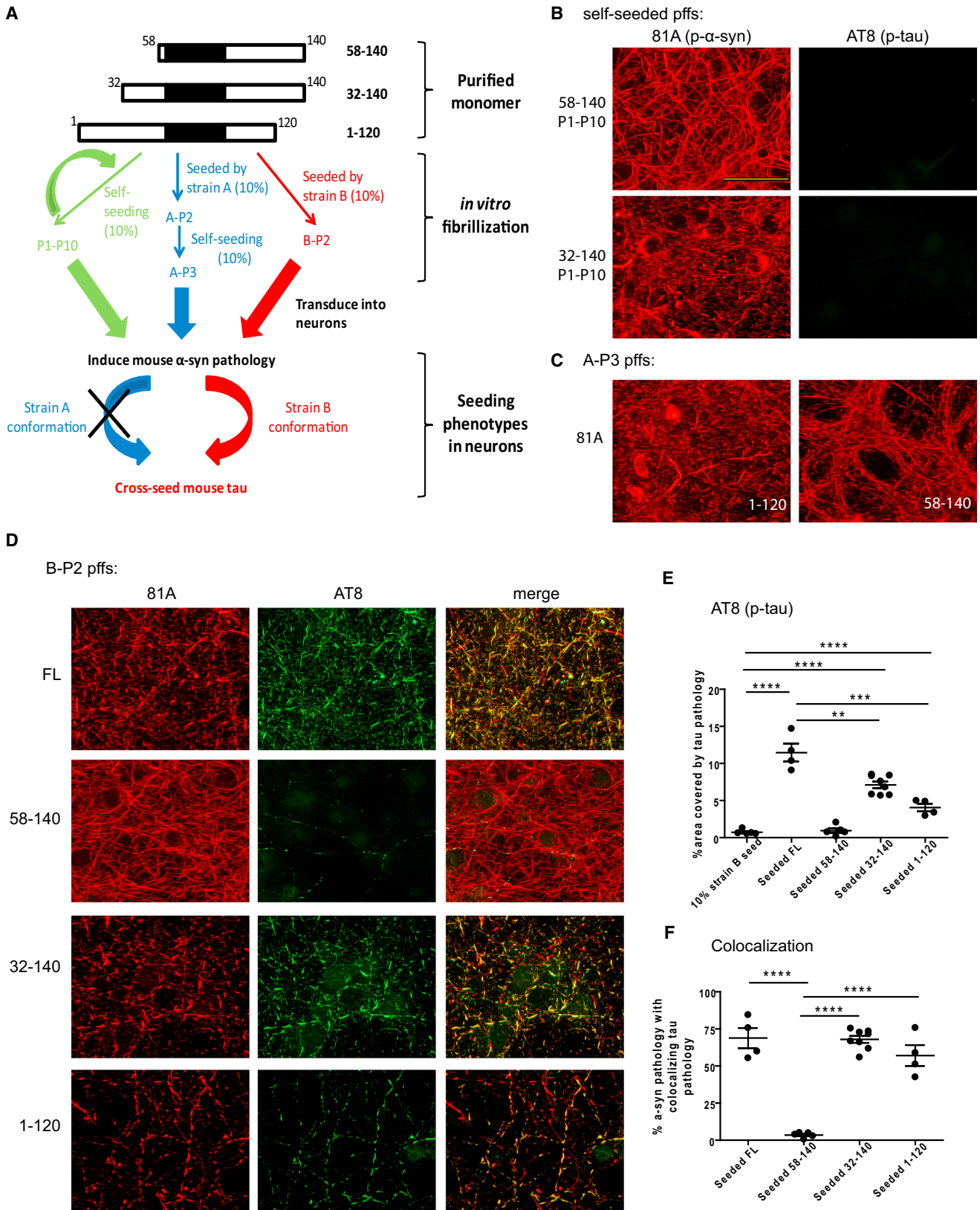
(legend on next page)

fibrillization of α-syn in the recipient neuron and our study showed that continual seeding in vitro can lead to evolution of α-syn strains, it is possible that transmission of α-syn pathology along multiple neuronal connections could also give rise to divergent pathological strains. This hypothesis could potentially account for morphologically different LBs in substantia nigra and neocortex, which are affected at different stages in the progression of PD and DLB (Braak et al., 2003; Kosaka et al., 1988).

Different strains of α-syn aggregates could also underlie the tremendous heterogeneity of synucleinopathies among different individuals (reviewed by Halliday et al., 2011). Whereas LBs and LNs are confined to neuronal perikarya and neurites for the majority of synucleinopathies, α-syn inclusions are largely confined to oligodendrocytes in multiple-system atrophy (Tu et al., 1998). PDD and DLB, which belong to a continuum of LB diseases, are clinically stratified according to the interval between the onset of motor symptoms and cognitive deficits that can vary by decades (Tsuboi and Dickson, 2005). Although comorbid AD pathologies are more common in DLB than in PDD, a bimodal distribution of neocortical NFTs has been found in DLB cases (Gearing et al., 1999). Furthermore, the presence of two subgroups of PDD patients has been described: one group has younger onset, long motor-dementia interval and relatively long disease duration, and the other group has older onset, short motor-dementia interval and more malignant disease course (Compta et al., 2011; Halliday et al., 2008). The former group usually presents with only LB pathologies, but the latter most often shows concomitant AD pathologies. Indeed, we detected conformational variants in sarkosyl-insoluble α-syn extracted from two subgroups of PDD patients with differential extent of concomitant AD pathologies, thus providing preliminary evidence for the existence of pathological α-syn strains in human synucleinopathy brains.

Prior to our study, the ability for a single molecule of the same primary sequence to adopt multiple fibril structures has been shown for a variety of amyloidogenic proteins other than prion protein, including Aβ (Kodali et al., 2010; Petkova et al., 2005), tau (Furukawa et al., 2011), and huntingtin with polyglutamine expansion (Nekooki-Machida et al., 2009), although the pathological relevance of amyloid fibril polymorphism other than cellular toxicity has never been investigated in cells or animals. The recently developed neuronal and animal models of pathology transmission allowed us to demonstrate distinct pathological seeding properties of specific α-syn fibril types generated in vitro. We speculate that perhaps besides interneuronal transmission of aggregated proteins, the existence of conformationally diverse protein strains underlying disease heterogeneity may be another common feature of neurodegenerative diseases; this feature was thought to be unique to prion diseases.

EXPERIMENTAL PROCEDURES

Recombinant α-Syn Purification and In Vitro Fibrillization

FL α-syn (1–140), N-terminal or C-terminal-truncated α-syn (32–140, 58–140, 1–120), and 1–120 with a C-terminal Myc-tag (1–120-Myc) were expressed in BL21 (DE3) RIL cells and purified as described (Giasson et al., 2001). Fibrillization was conducted by diluting recombinant α-syn to 5 mg/ml in Dulbecco's PBS (Cellgro, Mediatech Inc; pH adjusted to 7.0) and incubating at 37°C with constant agitation at 1,000 rpm for 5–7 days. Successful fibrillization was verified by sedimentation test and ThT-binding assay (see Extended Experimental Procedures). Pffs were stored at room temperature to avoid freeze and thaw.

Repetitive self-seeding was carried out by including 5% or 10% existing pffs (0.25 or 0.5 mg/ml in the final reaction) in a fibrillization reaction containing 95% or 90% fresh monomers (4.75 or 4.5 mg/ml in the final reaction) for generating the next passage of pffs, and the process was repeated until P10 (de novo pffs considered as P1) (Figure 1B). For fibrillization directly seeded by strain A or strain B pffs, 10% of existing pffs of either strain were added to a fibrillization reaction containing 90% fresh monomers. All seeded fibrillization was performed under the same conditions as de novo fibrillization. For each α-syn construct, at least two independently prepared monomer batches were tested for each fibrillization paradigm, and at least two series of self-seeded fibrillization were set up for each monomer batch.

Biophysical Analyses of α-Syn pffs

1–120-Myc α-syn strain A and B pffs were sonicated and diluted to a final concentration of 5 μM in 10 mM NaH$_2$PO$_4$, 100 mM KF buffer (pH 7.3). CD spectra were collected as described (Greenbaum et al., 2005). FL α-syn strain A and B pffs were spun at 100,000 × g for 15 min and resuspended in D$_2$O. This process was repeated two additional times, and then each sample was sonicated 50 times. FTIR spectra were collected as described earlier (Huang et al., 2002). See Extended Experimental Procedures for details.

PK Digestion of α-Syn pffs

Ten micrograms of pffs were mixed with 1 to 2.5 μg/ml of PK in Dulbecco's PBS to a final volume of 20 μl and incubated at 37°C for 30 min. Digestion was stopped with 1 mM PMSF. Reaction samples were boiled with SDS-sample buffer for 5 min and resolved on NuPAGE Novex 12% Bis-Tris gels (Invitrogen). To identify the N-terminal sequences of PK-resistant fragments, samples were transferred from 12% Bis-Tris gel to a sequencing-grade PVDF membrane, and individual bands were submitted to the Keck Biotechnology Resource Laboratory (Yale University) for N-terminal sequencing analysis. Epitope mapping of the PK digestion products was performed by immunoblotting samples that were transferred onto nitrocellulose membranes with epitope-specific antibodies to α-syn (Table S1).

Primary Neuron Cultures and Fibril Transduction

Primary neuron cultures were prepared from embryonic day (E) 15–E17 embryos of non-Tg CD1 mice (Charles River), α-syn knockout mice (Abeliovich et al., 2000), and homo/het crosses of PS19 mice (Yoshiyama et al., 2007). All procedures were performed according to the NIH Guide for the Care and Use of Experimental Animals and were approved by the University of Pennsylvania Institutional Animal Care and Use Committee (IACUC). Dissociated hippocampal neurons were plated onto poly-D-lysine-coated coverslips or dishes. Pff transduction was performed at 6 days or 7 days in vitro, whereby α-syn pffs

---

**Figure 5. The Roles of N and C Termini in Strain Conformations**

(A) Schematic diagram for testing the roles of N and C termini in generating or adopting strain A and B conformation.

(B) Pathology induced by de novo or self-seeded (P1–P10) 58–140 or 32–140 pffs in non-Tg neurons.

(C) Insoluble α-syn aggregates resulted from 1–120 or 58–140 pffs that were initially seeded by strain A pffs.

(D) Insoluble α-syn and tau aggregates induced by FL α-syn, 58–140, 32–140, or 1–120 pffs that were seeded by strain B pffs.

(E) Quantification of % area occupied by AT8-labeled tau pathology in (D) (independent preparations of pffs tested: n = 5 for 10% seed control, n = 4 for FL, n = 5 for 58–140, n = 8 for 32–140, n = 4 for 1–120; results shown as scatterplot with mean ± SEM. **p < 0.005; ***p < 0.0005; ****p < 0.0001).

(F) Calculation of % of α-syn pathology with colocalizing tau pathology in (D) (results shown as scatterplot with mean ± SEM, ****p < 0.0001).

For (B), (C), and (D), soluble proteins were removed during fixation. Scale bar: 50 μm. See also Figure S4 and Table S3.
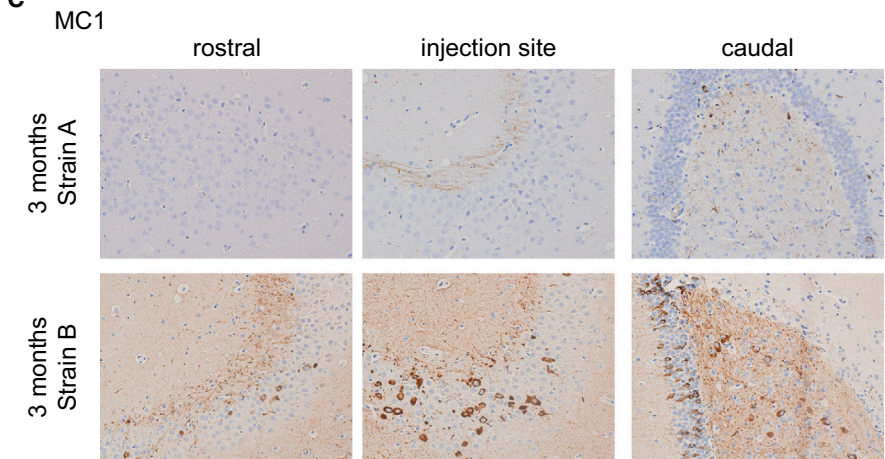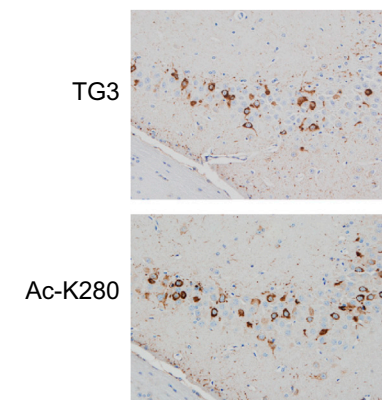
A

AT8

B

Rostral Hippocampus

Injection Site

Caudal Hippocampus

C

MC1
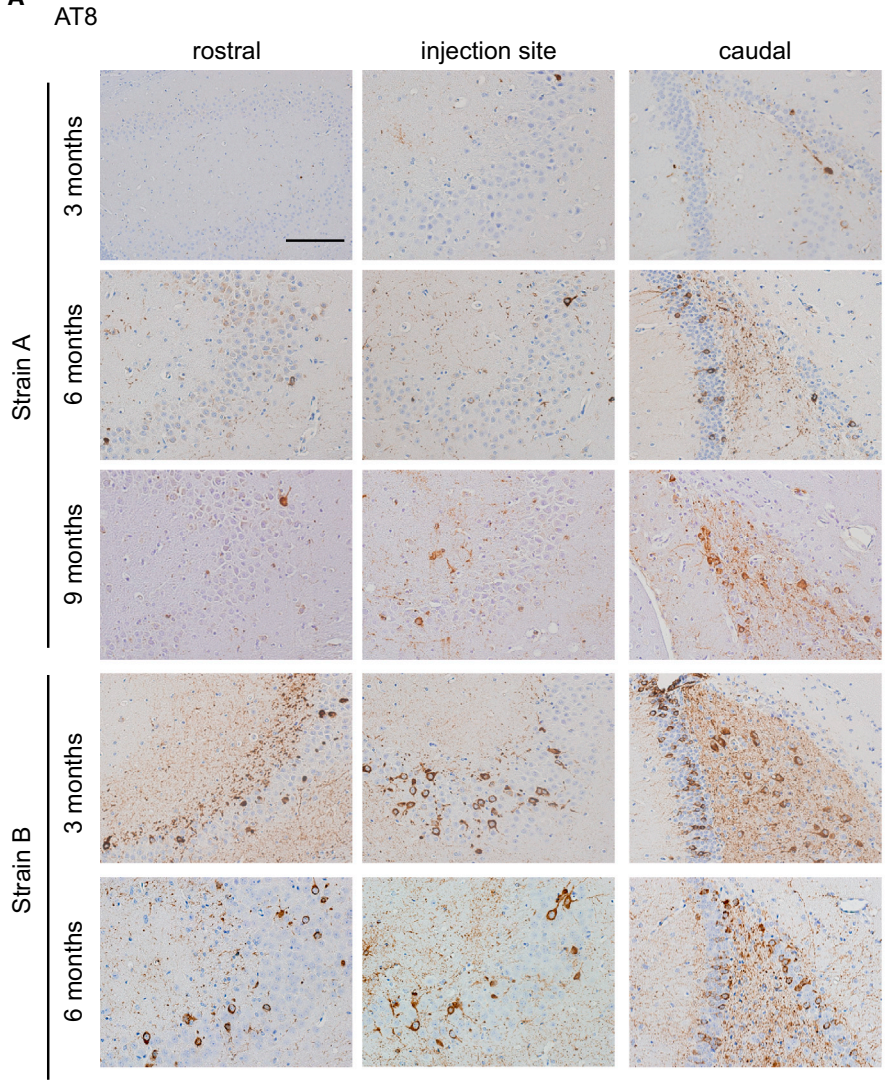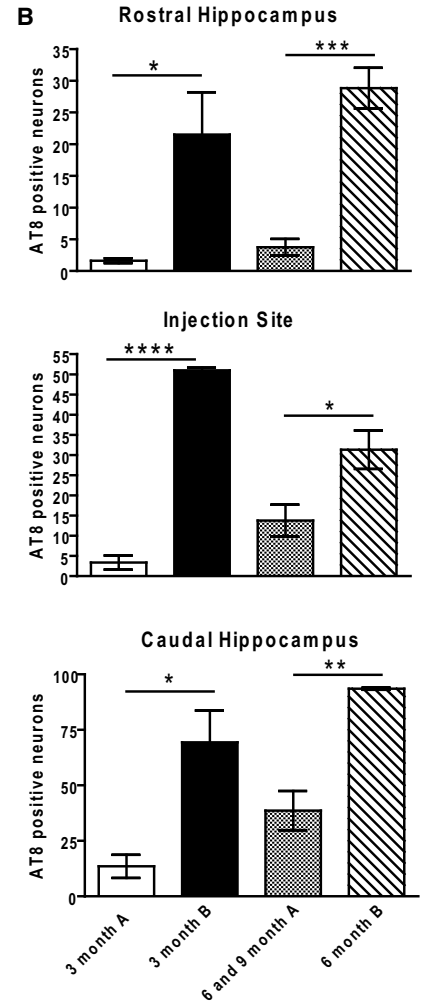
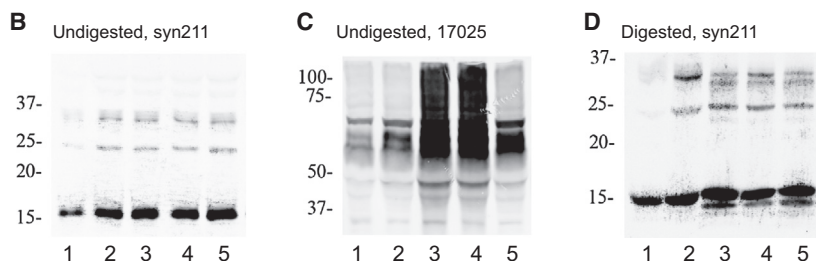**D** 3 months Strain B

(legend on next page)

A

Case No.	Primary Diagnosis	Secondary Diagnosis	Sex	Age at death	PMI (h)	Cingulate LB score	Cingulate NFT score
1	PDD	-	Male	59	10	3+	0
2	PDD	-	Male	70	12.5	3+	0
3	PDD	AD	Male	72	9	3+	2+
4	PDD	AD	Male	74	12	3+	3+
5	PDD	AD	Male	72	19	3+	1+

Figure 7. Conformational Variations of Pathological α-Syn in Synucleinopathy Brains

(A) Demographics of PDD cases used for pathological α-syn extraction from the cingulate gyrus. Primary and secondary diagnoses are based on neuropathological examination of postmortem brains. PMI: postmortem interval. Pathological scores of LBs and NFTs in the contralateral cingulate gyrus are shown, with "3+" being the highest score.

(B) Sarkosyl-insoluble fraction immunoblotted with mAb Syn211 showed abundant α-syn for all five cases.

(C) Sarkosyl-insoluble fraction from these five cases showed varying extents of tau accumulation revealed by pAb 17025.

(D) PK-digested sarkosyl-insoluble fraction showed different banding patterns of PK-resistant α-syn for PDD cases with or without abundant coexisting AD pathologies.

were diluted to 0.1 mg/ml in PBS and sonicated with 60 pulses before being added to neuron medium. For each 13 mm coverslip, 2 μg of pffs were added, and 8 μg of pffs were added per well for 6-well plates. Transduced neurons were harvested for immunocytochemistry or sequential extraction at time points indicated in the text (see Extended Experimental Procedures).

Cell-Survival Assays

LDH release assay and alamar blue assay were performed with CytoTox 96 Non-Radioactive Cytotoxicity Assay kit (Promega) and alamarBlue Cell Viability Assay kit (Invitrogen), respectively, according to the manufacturers' protocols (see Extended Experimental Procedures).

TEM and Immuno-EM

Negative-staining TEM of α-syn pffs and immuno-EM of transduced primary neurons were performed as previously described (Guo and Lee, 2011; Volpicelli-Daley et al., 2011). For double-labeling immuno-EM, goat anti-mouse IgG coupled to 10 nm colloidal gold and goat anti-rabbit IgG coupled to 6 nm colloidal gold (Electron Microscopy Sciences, Hatfield, PA, USA) were used to visualize primary antibodies against α-syn and tau, respectively. See Extended Experimental Procedures for details.

Antibody Generation and Application in Direct ELISA

HuA1 is an affinity-purified rabbit pAb raised against recombinant human α-syn. 9029-03 is a mouse mAb raised against strain B FL α-syn fibrils, and its conformational specificity was tested by direct ELISA, whereby 0.05–2 μg of sonicated α-syn fibrils of strain A or B were loaded into each well. For direct ELISA of different passages of α-syn fibrils, 0.5 μg of sonicated fibrils were loaded per well. For quantification, absorbance of wells incubated with 9029-03 was normalized to absorbance of corresponding wells incubated with HuA1. See Extended Experimental Procedures for details.

Stereotaxic Surgery and Immunohistochemistry

Unilateral inoculation of α-syn pffs into the hippocampus of 2- to 3-month-old PS19 mice or C57BL6/C3H F1 mice (Charles River) was performed using stereotaxic surgery as described (Iba et al., 2013) in accordance with protocols approved by the IACUC of the University of Pennsylvania. Immunohistochemical analysis of injected mice was conducted at 3, 6, and 9 months post-injection. See Extended Experimental Procedures for details.

PK Digestion of Sarkosyl-Insoluble Fraction from PDD Brains

Sarkosyl-insoluble fractions from the cingulate gyrus of PDD brains were prepared as described in the Extended Experimental Procedures, and the protein concentration was determined by bicinchoninic acid assay, so that equal amounts of total proteins were used for PK digestion across different samples, and PK concentration used was at a ratio of 3×10^{-3} to total protein concentration. Human brain extracts were incubated with PK at 37°C for 30 min, and reaction was stopped with 1 mM PMSF. Digested brain extracts were resolved on NuPAGE Novex 12% Bis-Tris gels (Invitrogen), whereas undigested samples were resolved on 4%–12% Bis-Tris gels.

Statistical Analysis

Two-tailed unpaired Student's t test was used for all the comparisons in the study, and differences with p values less than 0.05 were considered significant.

Figure 6. Strain-Specific Cross-Seeding of Tau Pathology In Vivo

(A) AT8-positive tau aggregates detected in different parts of ipsilateral hippocampus (rostral, near injection site, caudal) at 3, 6, or 9 months post-inoculation of strain A or B 1–120-Myc pffs into the hippocampus of PS19 mice.

(B) Quantification of AT8-positive neurons in different parts of ipsilateral hippocampus (n = 4 for 3 months post-injection of either strain, n = 4 for 6 or 9 months post-injection of strain A, n = 3 for 6 months post-injection of strain B; results shown as mean ± SEM. *p < 0.05; **p < 0.005; ***p < 0.0005; ****p < 0.00001).

(C) MC1 immunoreactivity in different parts of ipsilateral hippocampus at 3 months post-injection.

(D) tau inclusions cross-seeded by strain B pffs were recognized by TG3 and Ac-K280. All sections were counterstained with hematoxylin to reveal cell nuclei. Scale bar: 100 μm. See also Figure S5.

REFERENCES

Abeliovich, A., Schmitz, Y., Fariñas, I., Choi-Lundberg, D., Ho, W.H., Castillo, P.E., Shinsky, N., Verdugo, J.M., Armanini, M., Ryan, A., et al. (2000). Mice lacking alpha-synuclein display functional deficits in the nigrostriatal dopamine system. Neuron 25, 239–252.

Aguzzi, A., Heikenwalder, M., and Polymenidou, M. (2007). Insights into prion strains and neurotoxicity. Nat. Rev. Mol. Cell Biol. 8, 552–561.

Baba, M., Nakajo, S., Tu, P.H., Tomita, T., Nakaya, K., Lee, V.M., Trojanowski, J.Q., and Iwatsubo, T. (1998). Aggregation of alpha-synuclein in Lewy bodies of sporadic Parkinson's disease and dementia with Lewy bodies. Am. J. Pathol. 152, 879–884.

Ballatore, C., Lee, V.M., and Trojanowski, J.Q. (2007). Tau-mediated neurodegeneration in Alzheimer's disease and related disorders. Nat. Rev. Neurosci. 8, 663–672.

Braak, H., Del Tredici, K., Rüb, U., de Vos, R.A., Jansen Steur, E.N., and Braak, E. (2003). Staging of brain pathology related to sporadic Parkinson's disease. Neurobiol. Aging 24, 197–211.

Burré, J., Sharma, M., Tsetsenis, T., Buchman, V., Etherton, M.R., and Südhof, T.C. (2010). Alpha-synuclein promotes SNARE-complex assembly in vivo and in vitro. Science 329, 1663–1667.

Comellas, G., Lemkau, L.R., Nieuwkoop, A.J., Kloepper, K.D., Ladror, D.T., Ebisu, R., Woods, W.S., Lipton, A.S., George, J.M., and Rienstra, C.M. (2011). Structured regions of α-synuclein fibrils include the early-onset Parkinson's disease mutation sites. J. Mol. Biol. 411, 881–895.

Compta, Y., Parkkinen, L., O'Sullivan, S.S., Vandrovcova, J., Holton, J.L., Collins, C., Lashley, T., Kallis, C., Williams, D.R., de Silva, R., et al. (2011). Lewy- and Alzheimer-type pathologies in Parkinson's disease dementia: which is more important? Brain 134, 1493–1505.

Duda, J.E., Giasson, B.I., Mabon, M.E., Miller, D.C., Golbe, L.I., Lee, V.M., and Trojanowski, J.Q. (2002). Concurrence of alpha-synuclein and tau brain pathology in the Contursi kindred. Acta Neuropathol. 104, 7–11.

Frost, B., Jacks, R.L., and Diamond, M.I. (2009). Propagation of tau misfolding from the outside to the inside of a cell. J. Biol. Chem. 284, 12845–12852.

Furukawa, Y., Kaneko, K., and Nukina, N. (2011). Tau protein assembles into isoform- and disulfide-dependent polymorphic fibrils with distinct structural properties. J. Biol. Chem. 286, 27236–27246.

Galpern, W.R., and Lang, A.E. (2006). Interface between tauopathies and synucleinopathies: a tale of two proteins. Ann. Neurol. 59, 449–458.

Gearing, M., Lynn, M., and Mirra, S.S. (1999). Neurofibrillary pathology in Alzheimer disease with Lewy bodies: two subgroups. Arch. Neurol. 56, 203–208.

Giasson, B.I., Murray, I.V., Trojanowski, J.Q., and Lee, V.M. (2001). A hydrophobic stretch of 12 amino acid residues in the middle of alpha-synuclein is essential for filament assembly. J. Biol. Chem. 276, 2380–2386.

Giasson, B.I., Forman, M.S., Higuchi, M., Golbe, L.I., Graves, C.L., Kotzbauer, P.T., Trojanowski, J.Q., and Lee, V.M. (2003). Initiation and synergistic fibrillization of tau and alpha-synuclein. Science 300, 636–640.

Goedert, M. (2001). Alpha-synuclein and neurodegenerative diseases. Nat. Rev. Neurosci. 2, 492–501.

Goedert, M., Spillantini, M.G., Del Tredici, K., and Braak, H. (2013). 100 years of Lewy pathology. Nat. Rev. Neurol. 9, 13–24.

Gómez-Tortosa, E., Irizarry, M.C., Gómez-Isla, T., and Hyman, B.T. (2000). Clinical and neuropathological correlates of dementia with Lewy bodies. Ann. N Y Acad. Sci. 920, 9–15.

Greenbaum, E.A., Graves, C.L., Mishizen-Eberz, A.J., Lupoli, M.A., Lynch, D.R., Englander, S.W., Axelsen, P.H., and Giasson, B.I. (2005). The E46K mutation in alpha-synuclein increases amyloid fibril formation. J. Biol. Chem. 280, 7800–7807.

Guo, J.L., and Lee, V.M. (2011). Seeding of normal Tau by pathological Tau conformers drives pathogenesis of Alzheimer-like tangles. J. Biol. Chem. 286, 15317–15331.

Guo, J.L., and Lee, V.M. (2013). Neurofibrillary tangle-like tau pathology induced by synthetic tau fibrils in primary neurons over-expressing mutant tau. FEBS Lett. 587, 717–723.

Halliday, G., Hely, M., Reid, W., and Morris, J. (2008). The progression of pathology in longitudinally followed patients with Parkinson's disease. Acta Neuropathol. 115, 409–415.

Halliday, G.M., Holton, J.L., Revesz, T., and Dickson, D.W. (2011). Neuropathology underlying clinical variability in patients with synucleinopathies. Acta Neuropathol. 122, 187–204.

Huang, C.Y., Getahun, Z., Zhu, Y., Klemke, J.W., DeGrado, W.F., and Gai, F. (2002). Helix formation via conformation diffusion search. Proc. Natl. Acad. Sci. USA 99, 2788–2793.

Iba, M., Guo, J.L., McBride, J.D., Zhang, B., Trojanowski, J.Q., and Lee, V.M. (2013). Synthetic tau fibrils mediate transmission of neurofibrillary tangles in a transgenic mouse model of Alzheimer's-like tauopathy. J. Neurosci. 33, 1024–1037.

Ishizawa, T., Mattila, P., Davies, P., Wang, D., and Dickson, D.W. (2003). Colocalization of tau and alpha-synuclein epitopes in Lewy bodies. J. Neuropathol. Exp. Neurol. 62, 389–397.

Jicha, G.A., Bowser, R., Kazam, I.G., and Davies, P. (1997). Alz-50 and MC-1, a new monoclonal antibody raised to paired helical filaments, recognize conformational epitopes on recombinant tau. J. Neurosci. Res. 48, 128–132.

Jucker, M., and Walker, L.C. (2011). Pathogenic protein seeding in Alzheimer disease and other neurodegenerative disorders. Ann. Neurol. 70, 532–540.

Kayed, R., Head, E., Sarsoza, F., Saing, T., Cotman, C.W., Necula, M., Margol, L., Wu, J., Breydo, L., Thompson, J.L., et al. (2007). Fibril specific, conformation dependent antibodies recognize a generic epitope common to amyloid fibrils and fibrillar oligomers that is absent in prefibrillar oligomers. Mol. Neurodegener. 2, 18.

Kikis, E.A., Gidalevitz, T., and Morimoto, R.I. (2010). Protein homeostasis in models of aging and age-related conformational disease. Adv. Exp. Med. Biol. 694, 138–159.

Kodali, R., Williams, A.D., Chemuru, S., and Wetzel, R. (2010). Abeta(1-40) forms five distinct amyloid structures whose beta-sheet contents and fibril stabilities are correlated. J. Mol. Biol. 401, 503–517.

Kosaka, K., Tsuchiya, K., and Yoshimura, M. (1988). Lewy body disease with and without dementia: a clinicopathological study of 35 cases. Clin. Neuropathol. 7, 299–305.

Kotzbauer, P.T., Giasson, B.I., Kravitz, A.V., Golbe, L.I., Mark, M.H., Trojanowski, J.Q., and Lee, V.M. (2004). Fibrillization of alpha-synuclein and tau in familial Parkinson's disease caused by the A53T alpha-synuclein mutation. Exp. Neurol. 187, 279–288.

Lee, V.M., Goedert, M., and Trojanowski, J.Q. (2001). Neurodegenerative tauopathies. Annu. Rev. Neurosci. 24, 1121–1159.

Li, W., West, N., Colla, E., Pletnikova, O., Troncoso, J.C., Marsh, L., Dawson, T.M., Jäkälä, P., Hartmann, T., Price, D.L., and Lee, M.K. (2005). Aggregation promoting C-terminal truncation of alpha-synuclein is a normal cellular process and is enhanced by the familial Parkinson's disease-linked mutations. Proc. Natl. Acad. Sci. USA *102*, 2162–2167.

Luk, K.C., Song, C., O'Brien, P., Stieber, A., Branch, J.R., Brunden, K.R., Trojanowski, J.Q., and Lee, V.M. (2009). Exogenous alpha-synuclein fibrils seed the formation of Lewy body-like intracellular inclusions in cultured cells. Proc. Natl. Acad. Sci. USA *106*, 20051–20056.

Luk, K.C., Kehm, V., Carroll, J., Zhang, B., O'Brien, P., Trojanowski, J.Q., and Lee, V.M. (2012a). Pathological α-synuclein transmission initiates Parkinson-like neurodegeneration in nontransgenic mice. Science *338*, 949–953.

Luk, K.C., Kehm, V.M., Zhang, B., O'Brien, P., Trojanowski, J.Q., and Lee, V.M. (2012b). Intracerebral inoculation of pathological α-synuclein initiates a rapidly progressive neurodegenerative α-synucleinopathy in mice. J. Exp. Med. *209*, 975–986.

Miake, H., Mizusawa, H., Iwatsubo, T., and Hasegawa, M. (2002). Biochemical characterization of the core structure of alpha-synuclein filaments. J. Biol. Chem. *277*, 19213–19219.

Murphy, D.D., Rueter, S.M., Trojanowski, J.Q., and Lee, V.M. (2000). Synucleins are developmentally expressed, and alpha-synuclein regulates the size of the presynaptic vesicular pool in primary hippocampal neurons. J. Neurosci. *20*, 3214–3220.

Murray, I.V., Giasson, B.I., Quinn, S.M., Koppaka, V., Axelsen, P.H., Ischiropoulos, H., Trojanowski, J.Q., and Lee, V.M. (2003). Role of alpha-synuclein carboxy-terminus on fibril formation in vitro. Biochemistry *42*, 8530–8540.

Nekooki-Machida, Y., Kurosawa, M., Nukina, N., Ito, K., Oda, T., and Tanaka, M. (2009). Distinct conformations of in vitro and in vivo amyloids of huntingtin-exon1 show different cytotoxicity. Proc. Natl. Acad. Sci. USA *106*, 9679–9684.

O'Nuallain, B., and Wetzel, R. (2002). Conformational Abs recognizing a generic amyloid fibril epitope. Proc. Natl. Acad. Sci. USA *99*, 1485–1490.

Parchi, P., Castellani, R., Capellari, S., Ghetti, B., Young, K., Chen, S.G., Farlow, M., Dickson, D.W., Sima, A.A., Trojanowski, J.Q., et al. (1996). Molecular basis of phenotypic variability in sporadic Creutzfeldt-Jakob disease. Ann. Neurol. *39*, 767–778.

Petkova, A.T., Leapman, R.D., Guo, Z., Yau, W.M., Mattson, M.P., and Tycko, R. (2005). Self-propagating, molecular-level polymorphism in Alzheimer's beta-amyloid fibrils. Science *307*, 262–265.

Spillantini, M.G., Crowther, R.A., Jakes, R., Hasegawa, M., and Goedert, M. (1998). alpha-Synuclein in filamentous inclusions of Lewy bodies from Parkinson's disease and dementia with lewy bodies. Proc. Natl. Acad. Sci. USA *95*, 6469–6473.

Tsuboi, Y., and Dickson, D.W. (2005). Dementia with Lewy bodies and Parkinson's disease with dementia: are they different? Parkinsonism Relat. Disord. *11*(Suppl 1), S47–S51.

Tu, P.H., Galvin, J.E., Baba, M., Giasson, B., Tomita, T., Leight, S., Nakajo, S., Iwatsubo, T., Trojanowski, J.Q., and Lee, V.M. (1998). Glial cytoplasmic inclusions in white matter oligodendrocytes of multiple system atrophy brains contain insoluble alpha-synuclein. Ann. Neurol. *44*, 415–422.

Vilar, M., Chou, H.T., Lührs, T., Maji, S.K., Riek-Loher, D., Verel, R., Manning, G., Stahlberg, H., and Riek, R. (2008). The fold of alpha-synuclein fibrils. Proc. Natl. Acad. Sci. USA *105*, 8637–8642.

Volpicelli-Daley, L.A., Luk, K.C., Patel, T.P., Tanik, S.A., Riddle, D.M., Stieber, A., Meaney, D.F., Trojanowski, J.Q., and Lee, V.M. (2011). Exogenous α-synuclein fibrils induce Lewy body pathology leading to synaptic dysfunction and neuron death. Neuron *72*, 57–71.

Waxman, E.A., and Giasson, B.I. (2011). Induction of intracellular tau aggregation is promoted by α-synuclein seeds and provides novel insights into the hyperphosphorylation of tau. J. Neurosci. *31*, 7604–7618.

Weinreb, P.H., Zhen, W., Poon, A.W., Conway, K.A., and Lansbury, P.T., Jr. (1996). NACP, a protein implicated in Alzheimer's disease and learning, is natively unfolded. Biochemistry *35*, 13709–13715.

Witman, G.B., Cleveland, D.W., Weingarten, M.D., and Kirschner, M.W. (1976). Tubulin requires tau for growth onto microtubule initiating sites. Proc. Natl. Acad. Sci. USA *73*, 4070–4074.

Yoshiyama, Y., Higuchi, M., Zhang, B., Huang, S.M., Iwata, N., Saido, T.C., Maeda, J., Suhara, T., Trojanowski, J.Q., and Lee, V.M. (2007). Synapse loss and microglial activation precede tangles in a P301S tauopathy mouse model. Neuron *53*, 337–351.